

Supporting Information

Superparamagnetic Ellipsoid Nanoclusters from Emulsion Electrospinning

Markus B. Bannwarth^{†}, Agathe Camerlo[†], Sebastian Ulrich^a, Gerhard Jakob[‡], Giuseppino Fortunato[†], René M. Rossi[†], Luciano F. Boesel^{†*}*

[†]Empa, Laboratory for Protection and Physiology, Lerchenfeldstrasse 5, CH-9014 St. Gallen, Switzerland.

[‡]Institute of Physics, University of Mainz, Staudingerweg 7, 55128 Mainz, Germany.

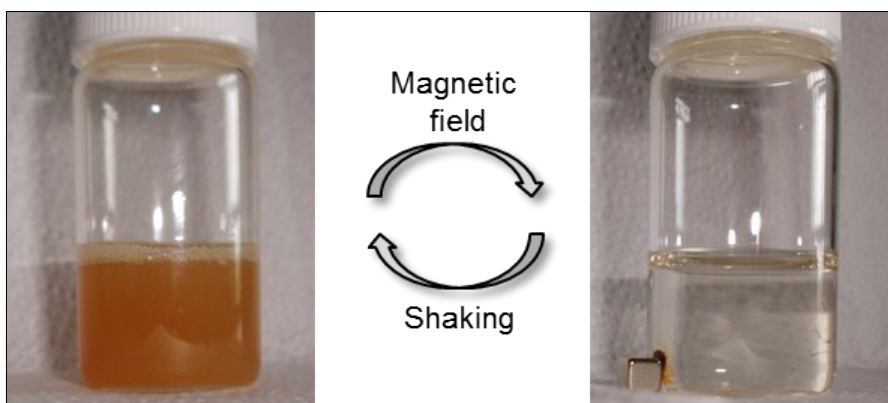


Figure S1. *Optical micrograph showing the response of ESIONCs upon application of an external magnetic field applied by a small permanent magnet. When putting the permanent magnet next to a dispersion of ESIONCs, they can be easily collected next to the magnet due to their high saturation magnetization when applying the external magnetic field.*

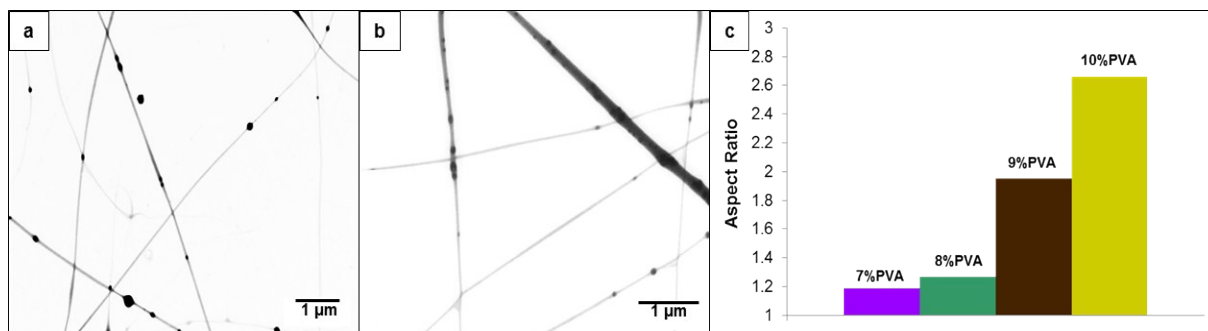


Figure S2. STEM images of fibers containing iron oxide nanoclusters. The fibers were formed from aqueous emulsions with different PVA concentrations: 3 and 7 wt.% in Figure a and b, respectively. Figure c shows the dependency of the average aspect ratio with the PVA concentration

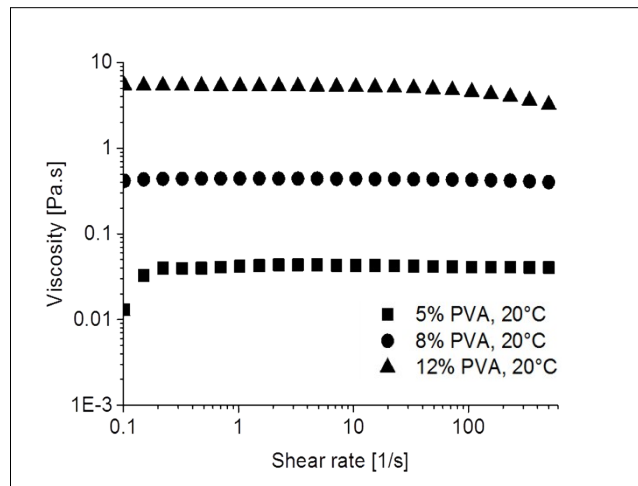


Figure S3. *Viscosity of aqueous PVA solutions of 5, 8, and 12 wt.% at different shear rates.*

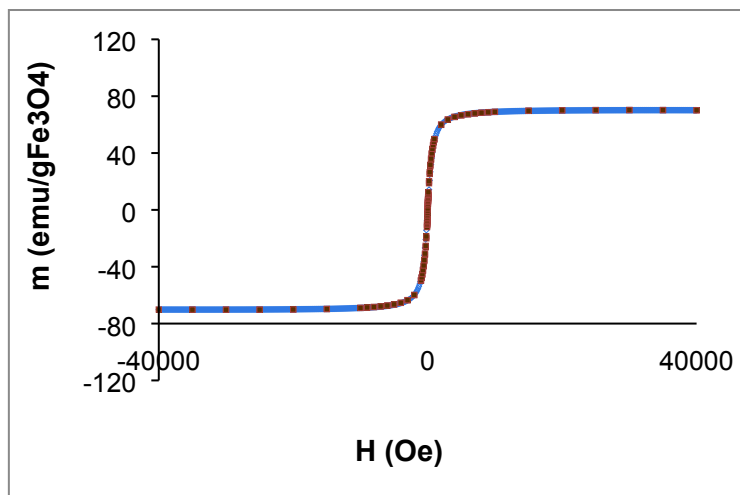


Figure S4. SQUID magnetization curve of ESIONCs as experimentally measured (\square) and theoretically calculated (\diamond).

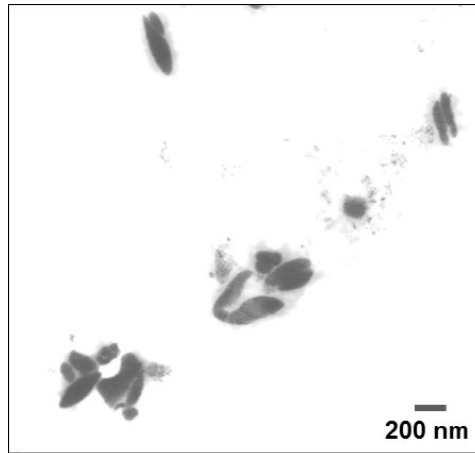


Figure S5. *STEM image of ESIONCs that were treated as aqueous dispersion for 1 min in an ultrasonication bath. Most of the ESIONCs maintain their ellipsoid shape. However, one can observe the beginning of a degradation/decomposition process of the ESIONCs.*

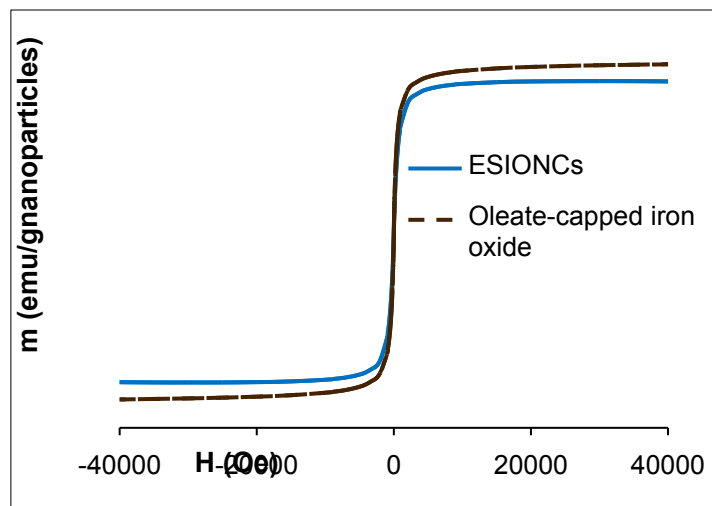


Figure S6. VSM curves of the spherical oleate-capped iron oxide nanoparticles before electrospinning and the ESIONCs. Both curves follow the same trend, showing no observable remanence. The saturation magnetization of the original, spherical oleate-capped iron oxides is slightly higher in comparison to the magnetization of the ESIONCs. This small difference can be explained by the PVA layer which sticks to the ESIONCs after electrospinning in the PVA solution. The PVA reduces the percentage of superparamagnetic iron oxides per particle and hence the saturation magnetization per gram of particles.

Experimental

Methods

SEM and STEM were performed on a Hitachi S-4800 (Hitachi High technologies, Canada). SEM samples were drop-casted on a silicon wafer and sputtered with gold (Polaron Equipment, SEM coating Unit E5100, Kontron AG, Switzerland, 5 nm thick coating). STEM samples were drop-casted on a 300 mesh carbon coated copper grid. Solid contents were calculated from gravimetric data.

X-ray powder diffraction (XRD) patterns were obtained using a PANalytical X'Pert PRO θ - 2θ scan system equipped with a Johansson monochromator (Cu-K α_1 radiation, 1.5406 Å) and an X'Celerator linear detector. The diffraction pattern was recorded between 20° and 80° (2 θ) with an angular step interval of 0.0167°.

Magnetic properties of the ESIONCs were determined *via* a Superconducting Quantum Interference Device (SQUID) magnetometer (Quantum Design MPMS XL). The sample material was measured in a gelatin capsule, which provides a negligible purely diamagnetic background signal. The corresponding data is depicted in Figure S4. The simulated magnetization curve in Figure S4 results from the superparamagnetic response of Fe₃O₄ particles with a total spin momentum of J=S=6900 and a diamagnetic contribution of $\chi_{\text{dia}} = -1.942 \cdot 10^{-5} \text{ emu} \cdot (\text{g} \cdot \text{Oe})^{-1}$ from the sample holder and organic shell material. As magnetite provides 4 μ_B ·f.u.⁻¹ (Bohr magnetons per formula unit), approximately 3450 f.u. are contained in each nanoparticle corresponding to a diameter of a spherical nanoparticle of 7.85 nm. Since the simulated curve stems from a unique small particle size, it is obvious that the clustered ellipsoids show the magnetic response of the individual contributing nanoparticles in this hysteresis curve. Nevertheless, shape anisotropy due to the ellipsoidal clusters can lead to additional demagnetization effects not present in the simulation. Also the outermost shell of a magnetic nanoparticle shows usually a reduced magnetic response due to the different chemical surrounding. Thus, the particle size calculated from the total spin moment is a lower boundary of the true value. On the other hand, the high value measured for the saturation magnetization limits the thickness of a nonmagnetic shell to smaller than 0.3 nm, i.e. less than the length of a cube containing one formula unit. For the latter estimation we compared to the temperature dependence of the saturation magnetization as measured in bulk single crystals.¹ The diameter of the superparamagnetic particles can therefore be estimated to be around 8.5 nm (core + weak magnetic outer shell), which is roughly consistent with the average crystallite size of ~10 nm as determined from XRD measurements by using the Scherrer equation.

For determination of the blocking temperature, the sample was cooled to 10 K. A field of 150 Oe was applied and measurements were taken during warming to 300 K with a rate of 2.5 K·min⁻¹ (zfc). Afterwards, measurements were taken during cooling to 10 K in the

applied field (fc). Finally the data was measured during warming without changing the magnetic field (fw). The field warming and field cooling curves are practically identical and form the upper branch of Figure 4e, while the zero field curve is the lower branch.

TGA analysis was performed on a NETZSCH TG 209 F1 instrument under nitrogen atmosphere from 25-800 °C with a heating rate of 10 K·min⁻¹. A rheometer (Anton Paar Physica MCR 300, Austria) equipped with a plate - cone geometry was applied in controlled shear rate mode to assess the shear viscosities as a function of shear rate. Flow curves with shear rates varying from 0.01 - 500 s⁻¹ were recorded at 20 °C.

Synthesis of Oleate-Capped Iron Oxide Nanoparticles

All commercially available reagents and solvents were used without further purification. The synthesis of oleate-capped iron oxide nanoparticles was done as similar reported in literature.^{2, 3} Briefly, a 90 mmol FeCl₃·6H₂O and 60 mmol FeCl₂·4H₂O were dissolved in 100 mL of demineralized water. 40 mL of an ammonium hydroxide solution (28% NH₃ in water) were added dropwise before adding 15 mmol oleic acid. Under vigorous stirring, the reaction was kept at 70 °C for 1 h and at 100 °C for 2 h while constantly refilling the evaporating water with deionized water. After complete evaporation of excess NH₃, the reaction mixture was cooled to room temperature and put on top of a permanent magnet to precipitate the magnetic nanoparticles. The particles were washed several times with deionized water and dried under vacuum before further use.

Preparation of Miniemulsion Droplets Containing Iron Oxide Nanoparticles

For the formation of iron oxide containing miniemulsion droplets, 4 g of oleate-capped iron oxide nanoparticles were redispersed in 4 g of *n*-octane in an ultrasonication bath for 1 h. The resulting black dispersion was mixed with 24 g of water containing 24 mg of SDS and stirred for 1 h at 1400 rpm to form a macro emulsion. Miniemulsion droplets were formed by ultrasonication under ice cooling using a Branson Digital Sonifier with ½ inch ultrasonication tip (3 min, 50% amplitude, 10 s pulse, 5 s pause).

Emulsion Electrospinning of the Iron Oxide Containing Miniemulsion

The iron oxide containing miniemulsion was mixed non-magnetically over night with an aqueous solution containing 15 wt.% Poly (vinyl alcohol) (M_w = 205.000 g·mol⁻¹) to form a 10 wt.% PVA miniemulsion and filled into a 1 mL syringe. When bubbles were present in the syringe, they were removed by putting the syringe in an ultrasonication bath. Emulsion electrospinning was then performed *via* a previously described electrospinning setup,^{4, 5} which was placed in a climate chamber to have good control over the spinning conditions. The emulsion was then spun at 24 °C and at a relative humidity of 60% (20 cm distance, 7 μL·min⁻¹ feed rate, 0.8 mm tip diameter, +12 and -5 V and 0.1 mA) and the fibers collected

on top of an aluminum foil or on a carbon coated copper grid. The fibers were analyzed *via* SEM and STEM.

Dissolution of PVA Fibers and Subsequent Dispersion of Elongated Iron Oxide Nanoclusters

For dissolution of the elongated nanoparticles, the fiber mesh was removed from the aluminum foil and demineralized water added. After shaking for 5 min, the magnetic dispersion was put on top of a permanent magnet until most of the particles settled on the magnet. The supernatant was discarded and refilled with deionized water. Then the particles were analyzed by SEM, STEM, SQUID magnetometry and TGA.

1. Özdemir, Ö., Coercive force of single crystals of magnetite at low temperatures. *Geophysical Journal International* **2000**, *141*, 351-356.
2. Bannwarth, M. B.; Kazer, S. W.; Ulrich, S.; Glasser, G.; Crespy, D.; Landfester, K., Well-Defined Nanofibers with Tunable Morphology from Spherical Colloidal Building Blocks. *Angew. Chem. Int. Ed.* **2013**, *52*, 10107-10111.
3. Bannwarth, M. B.; Weidner, T.; Eidmann, E.; Landfester, K.; Crespy, D., Reversible Redox-Responsive Assembly/Disassembly of Nanoparticles Mediated by Metal Complex Formation. *Chem. Mater.* **2014**, *26*, 1300-1302.
4. Camerlo, A.; Vebert-Nardin, C.; Rossi, R. M.; Popa, A. M., Fragrance encapsulation in polymeric matrices by emulsion electrospinning. *Eur. Polym. J.* **2013**, *49*, 3806-3813.
5. Fortunato, G.; Guex, A. G.; Popa, A. M.; Rossi, R. M.; Hufenus, R., Molecular weight driven structure formation of PEG based e-spun polymer blend fibres. *Polymer* **2014**, *55*, 3139-3148.